

Full Length Research Paper

Utilization of Co-Zeolite imidazolate frameworks (Co-ZIF) as catalyst for organic transformations

Adewale OLAMOYESAN^{1*}, Jiexiang WANG¹, Hua ZHANG¹, Yu DENG, Bodunde Joseph OWOLABI² and Binghui CHEN¹

¹College of Chemistry and Chemical Engineering, National Engineering Laboratory for Green Chemical Productions of Alcohols–Ethers–Esters, Xiamen University, Xiamen 361005, China.

²Federal University of Technology Akure, P. M. B 704 Akure, Ondo State, Nigeria.

Received 24 April, 2014; Accepted 5 June, 2014.

An excellent conversions of benzaldehyde was obtained under solvent and solvent free conditions by utilizing Co(im)₂0.5 DMA as catalyst for the synthesis of benzylidene malononitrile. The catalytic prospect of this crystalline porous framework was extended to oxidation reactions involving ethylene glycol (EG) and ethylbenzene (EB). Unexpectedly, EG was totally oxidized to oxalic acid; which demonstrates the catalyst non-selectivity towards glycolic acid. For EB oxidation under a solvent less condition in the presence of oxygen as oxidant (0.8 Mpa), and a 42% conversion was achieved with 78.4% selectivity for acetophenone at 120°C for a period of 2 h.

Key words: Metal-organic frameworks, zeolitic imidazolate frameworks, ethylene glycol, ethylbenzene.

INTRODUCTION

The next phase after the substantial foundation of metal-organic frameworks (MOFs) synthetic chemistry is the utilization of its chemical versatility and functionality. MOFs have been identified for prospective applications in gas separation and storage, sensors, drug delivery and catalysis (Czaja et al., 2009; Yilmaz et al., 2011; Kuppler et al., 2009; Shekhah et al., 2011). These crystalline frameworks functionalities for catalysis can arise from: metal ions, organic linkers, the pore sites, encapsulated active sites (Corma et al., 2010). The self supporting strategy offers by this class of materials have shown to be effective in a number of different reactions with

various coordination complexes (Corma et al., 2010; Lee et al., 2009; Gascon et al., 2014), and have also provided a desirable environmentally benign and selective catalytic process. MOFs as other heterogeneous catalysts are advantageous for liquid phase organic transformation as they are easily recoverable with minimal environmental impact (Ma and Lin, 2010).

Zeolite imidazolate frameworks (ZIFs), a sub class of this porous material; where its crystal structures share the same topologies as those that can be found in zeolites, were chosen for the catalytic exploration and evaluation on the basis of its thermal and chemical

*Corresponding author. E-mail: adewale.olamoyesan@gmail.com. Tel: +2348179912978.

Author(s) agree that this article remain permanently open access under the terms of the [Creative Commons Attribution License 4.0 International License](http://creativecommons.org/licenses/by/4.0/)

stability (Park et al., 2006). Till date, only a few examples of the potential of ZIFs as catalysts have been recently published: ZIF-8 catalyzes the trans-esterification of vegetable oil (Chizallet et al., 2010); and is an active catalyst for the Knoevenagel reaction (Tran et al., 2011); also ZIF-9 has been used as a catalyst in the oxidation of aromatic oxygenates (Zakzeski et al., 2011), and for C-C coupling reaction (Nguyen et al., 2012); ZIF-8 catalyzes the conversion of CO₂ to chloropropene carbonate (Miralda et al., 2012) and for synthesis of ethyl methyl carbonate (Zhou et al., 2013); the most recent is Au@ZIF-8 and Au@ZIF-90 for aerobic oxidation of benzyl alcohol (Aijaz and Xu, 2014).

Indeed, in this direction we decide to explore and evaluate the catalytic prospect of Co-ZIFs for; Knoevenagel condensation of benzaldehyde with malononitrile, oxidation of ethylene glycol and ethylbenzene, where the ligand catalyses the condensation and the metal ion (Co²⁺) for oxidation transformation of the substrates of interest.

EXPERIMENTAL

Materials

Cobalt nitrate hexahydrate (99.50%), Benzaldehyde (98.50%), Malononitrile (99.00%), Ethylene glycol (99.00%), Ethylbenzene (98.50%), N,N-dimethylacetamide (DMA) (99.50%), N,N-dimethylformamide (DMF) (99.50%), Dichloromethane (DCM) (99.50%) and Piperazine (99.00%) were purchased from Sinopharm Chemical Reagent, China. These chemicals were used without further purification.

Preparation of Co-ZIFs

Synthesis of [Co(im)₂0.5 DMA]_n (1)

Co(im)₂0.5 DMA was synthesized based on the procedure reported by Tian et al. (2004) Co(NO₃)₂·6H₂O (3.638 g, 0.0125 mol), C₃H₄N₂ (1.7 g, 0.025 mol), and piperazine (1.075 g, 0.0125 mol) were dissolved in DMA (65 mL). The reaction mixture was stirred at room temperature for 2 h. Then the solution was then placed in a Teflon-lined autoclave and heated in an oven at 135°C and maintained at 135°C for 24 h. After unassisted cooling to room temperature, the violet crystals were collected and washed with DMA (30 mL) with a yield of ~45% based on imidazolate ligand.

Synthesis of Co(im)₂0.5DMF (2)

Co(NO₃)₂·6H₂O (3.64 g, 0.0125 mol) and C₃H₄N₂ (2.35 g, 0.345 mol) were added to DMF (60 mL). The reaction mixture was stirred at room temperature for 12 h. Then the solution was placed in a Teflon-lined autoclave and heated in an oven at 140°C and maintained at 140°C for 48 h. After unassisted cooling to room temperature, the violet crystals were collected and washed with DMF (30 mL) with a yield of ~25% based on imidazolate ligand.

Synthesis of Co(nim)₂ (3)

Co(NO₃)₂·6H₂O (2.183 g, 7.5 mmol) and 4-nitroimidazole, C₃H₃N₃O₂ (8.482 g, 75 mmol) were added to DMF (30 mL). The reaction

mixture was stirred at room temperature for 12 h. Then, the solution was placed in a Teflon-lined autoclave and heated in an oven and maintained at 120°C for 24 h. After cooling to room temperature, the cube-shaped single crystals were collected and washed with DMF (30 mL).

Characterization of Co-ZIFs

The single crystal data were collected on a Bruker SMART APEX CCD diffractometer with graphite monochromated Mo K α radiation ($\lambda = 0.71073 \text{ \AA}$) radiation. Powder XRD patterns of the samples were recorded on a Phillips X'Pert Pro Super X-ray diffractometer equipped with X'Celerator detection system and CuK α radiation (40 kV and 30 mA) was used as the X-ray source. Scans were performed over the 2θ range from 5 to 45°, using a resolution of 0.028° in a step size of the 0.0167° and counting of 10 s per step. The morphology of the samples was observed by a field-emission scanning electron microscope (FESEM, LEO-1530, Germany) combined with energy dispersive spectroscopy (EDS) and Olympus optical microscopy. Fourier transform infrared (FT-IR) measurements were recorded on a Nicolet 740 FTIR spectrometer at ambient conditions. TG-DTA was carried out in static air using a SDT Q600 V20.9 Build 20 thermal analyzer in the temperature range 30 to 800°C at a heating rate of 10°C min⁻¹. The UV-vis spectra were recorded on a Shimadzu 1750 UV-vis Spectrophotometer at room temperature.

Catalytic activity

Typical procedure for the Knoevenagel condensation reaction

Inspired by the principle of green chemistry, the initial reaction was carried out in a solvent free environment and at room temperature. The Knoevenagel reaction between benzaldehyde and malononitrile using Co(im)₂0.5 DMA as catalyst was carried out in a batch-wise 25-ml round-bottom flask magnetically stirred. A mixture of benzaldehyde (5.16 ml, 0.05 mol), and malononitrile (3.03 g, 0.05 mol) was placed into the flask and stirred for 2 min; thereafter 0.295 g, 5 mmol of catalyst was added to the reaction mixture. The catalyst concentration was calculated with respect to the cobalt/benzaldehyde molar ratio. The reaction vessel was continuously stirred until the completion of the reaction, where the porous crystal solid absorbed all the solvent and formed a sticky amorphous brown gel after 5 min. After the completion of the reaction, the product was obtained with the addition of 10 ml DCM, and then the solid cobalt imidazolate framework was separated from the mixture by simple centrifugation and then followed by filtration when necessary; for reusability sake, the catalyst was washed with copious amount of DCM dried under vacuum at 60°C for 12 h. The reaction mixture was analyzed by Shimadzu GC 2010, filtered through a short silica gel pad, analyzed by GC and the product identity was confirmed by GC-MS when necessary.

Gas chromatographic (GC) analyses were performed using a Shimadzu GC 2010 equipped with a flame ionization detector (FID) and a DB-35 column (length = 60 m, inner diameter = 0.25 mm, and film thickness = 0.25 μm). The temperature program for GC analysis was kept at 70°C for 6 min and heated samples from 70 to 280°C at 5°C/min and were held at 280°C for 15 min. Injector and detector temperatures were set constant at 280°C with a column flow rate of 2.0 mL⁻¹.

Typical procedure for the oxidation of ethylene glycol

The investigation of possible oxidation of ethylene glycol into less toxic or useful products such as glycolic acid was carried out in a

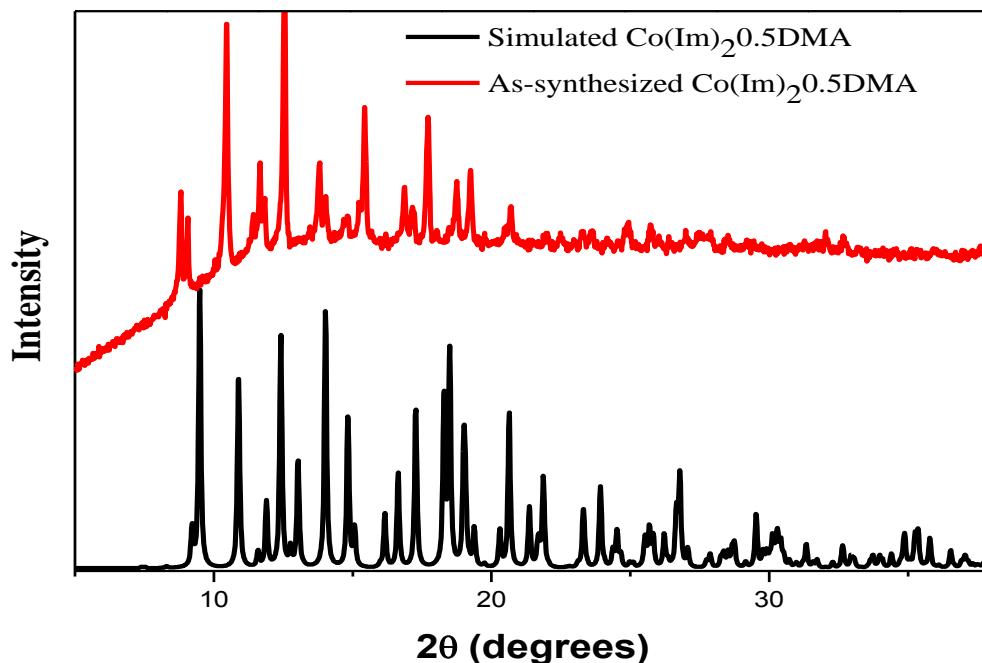


Figure 1. Comparison of the experimental PXRD of as-synthesized $\text{Co}(\text{im})_2\text{0.5DMA}$ with the simulated pattern from its single crystal structure.

300 ml Parr reactor (550 series). Ethylene glycol, NaOH (50 mmol) and the catalyst (metal/reactant = 10^{-3}) were mixed with distilled water to a total volume of 100 ml. The reaction mixture was charged into the autoclave, exchanged three times with pure oxygen, pressurized with O_2 to 300 KPa, and then stirred and heated to appropriate temperature. After the reaction mixture was cooled to room temperature, the excess gas was vented, the resultant liquid was taken out and the catalyst was separated from the mixture by simple filtration. The aqueous solution was analyzed by a Dionex Ultimate U3000 HPLC system, equipped with online degasser, dual gradient pump (loading pump and analytical pump), an auto sampler with a 100 μL sample loop, a column oven, and a diode array detector. The Chroméléon software (Dionex, Sunnyvale, USA) was used to control the system to collect data. A reversed phase column of Acclaim $\text{\textcircled{R}}$ Polar Advantage II (PA II) C18 (150 mm \times 4.6 mm, 5 μm) was used with aqueous 0.01 M H_2SO_4 (0.8 ml/min) as the eluent. Samples of reaction mixture (0.1 ml) were diluted (10 ml) by using the eluent.

Typical procedure for the oxidation of ethylbenzene

The heterogeneous catalytic oxidation reaction was performed in 100 ml stainless steel reactor. Ethylbenzene (98.50%) was used as obtained without any further purification, and the as-synthesized catalyst with DMA guest molecule was exchanged by dichloromethane (DCM) (3 \times 15 ml) for 3 days; thereafter the residual solvents were removed under vacuum at 200°C for 6 h. In a typical experimental procedure, ethylbenzene (30 ml, 0.4 mol) and cobalt imidazolate framework $\text{Co}(\text{im})_2\text{0.5DMA}$ (0.928 g, 0.04 mol) were added into the 100 ml autoclave, exchanged three times with pure oxygen, filled with O_2 to 0.8×10^6 Pa, stirred and heated to 120°C for a period of 2 h. After the reaction mixture was cooled to room temperature in a bath of ice/water mixture, excess gas was vented, resultant liquid was taken out and solid catalyst was separated from the mixture by simple centrifugation followed

by filtration when necessary; for reusability sake the catalyst was washed with copious amount of DCM dried under vacuum at 60°C for 12 h.

The filtrate was analyzed with Shimadzu GC 2010, filtered through a short silica gel pad and the product identity was confirmed by Gas chromatography–mass spectrometry (GC-MS). Gas chromatographic (GC) analyses were performed using a Shimadzu GC 2010 equipped with a flame ionization detector (FID) and a AT-SE 30 column (length = 30 m, inner diameter = 0.25 mm, film thickness = 0.33 μm). The temperature program for GC analysis started from 40 to 200°C at 10°C/min, kept at 200°C for 10 min, heated from 200 to 280°C and held at 280°C for 2 min. Injector and detector temperatures were set constant at 200 and 280°C, respectively with a column flow rate 2.0 ml^{-1} .

RESULTS AND DISCUSSION

Characterization of the catalysts

There exist high degrees of correspondence between the experimental and simulated XRD patterns for both $\text{Co}(\text{im})_2\text{0.5DMA}$ and $\text{Co}(\text{im})_2\text{0.5DMF}$ as shown in (Figures 1 and 2); which is an indication that the bulk material is a true representation of the single crystal. On the other hands, the powder pattern simulated $\text{Co}(\text{im})_2$ revealed three clearly observable peaks and several weak reflections in the range of 2θ (12 to 40°), which are not visible on the experimental pattern (Figure 3). The observed difference in diffractograms could be attributed to the preferred orientation of growth during $\text{Co}(\text{im})_2$ synthesis. An apparent decline in the intensity of the peaks were observed for used $\text{Co}(\text{im})_2\text{0.5DMA}$ catalyst

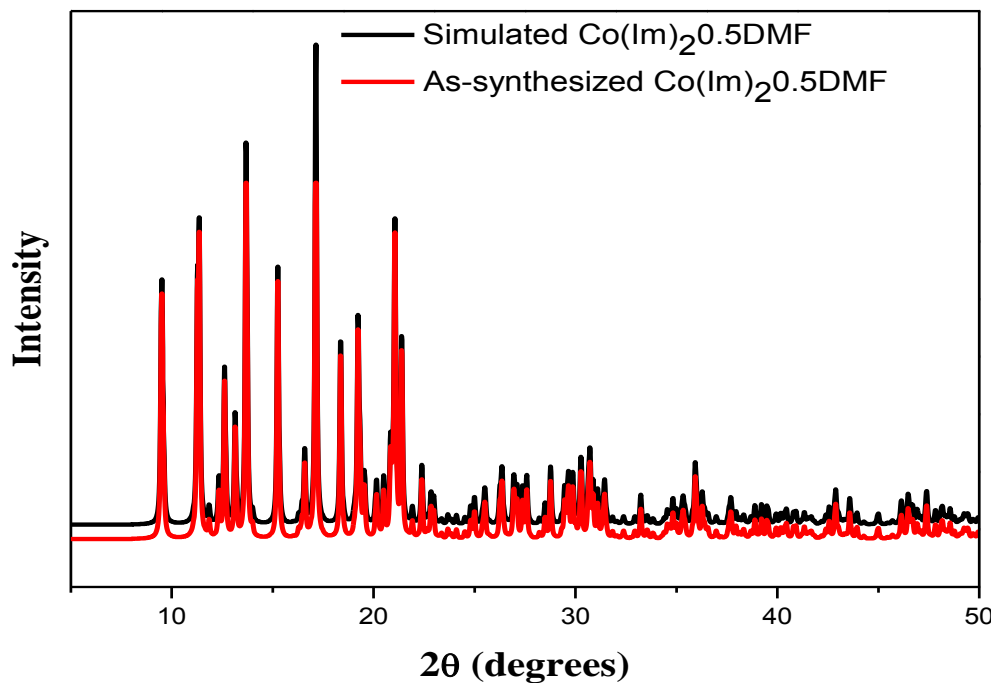


Figure 2. Comparison of the experimental PXRD of as-synthesized $\text{Co}(\text{im})_2 \cdot 0.5\text{DMF}$ with the simulated pattern from its single crystal structure.

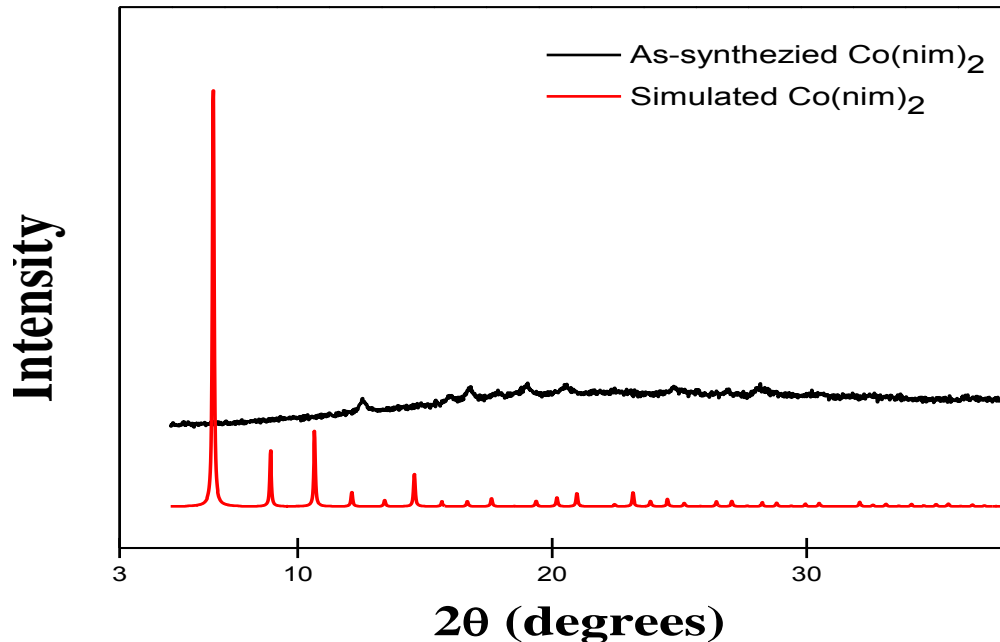


Figure 3. Comparison of the experimental PXRD of as-synthesized $\text{Co}(\text{nim})_2$ with the simulated pattern from its single crystal structure.

and this was most significant for Knoevenagel condensation (Figure 4), where the crystalline material transformed to sticky amorphous. Noteworthy, the

catalytic active site of this porous crystal material was retained during the course of rerun experiments, and consistent conversions were obtained for the reusability

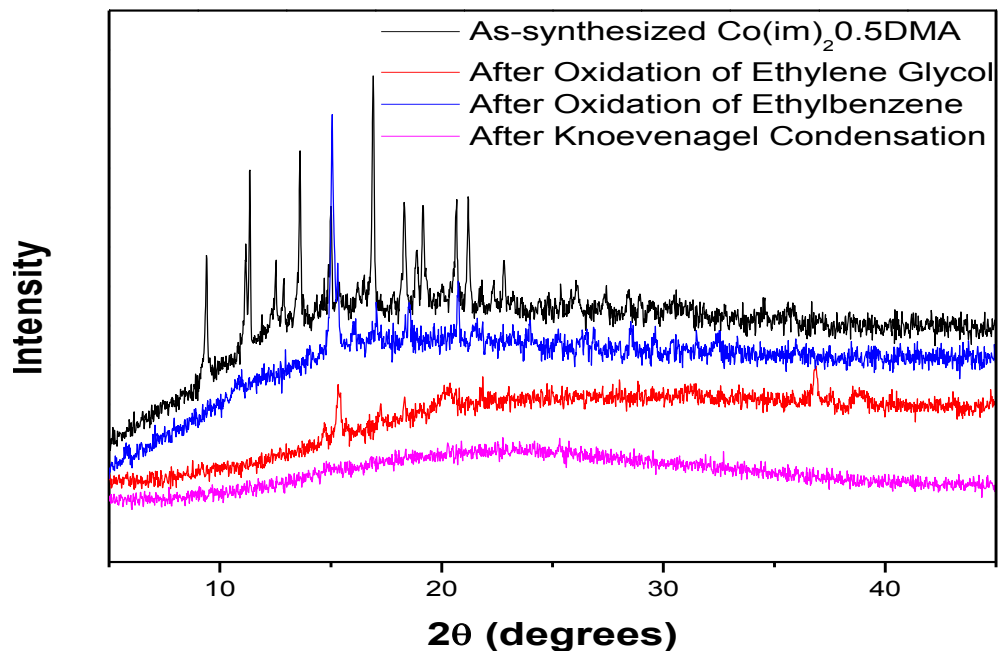


Figure 4. Comparison of PXRD pattern of fresh $\text{Co}(\text{im})_2 \cdot 0.5\text{DMA}$ and after usage for specific organic synthesis reaction.

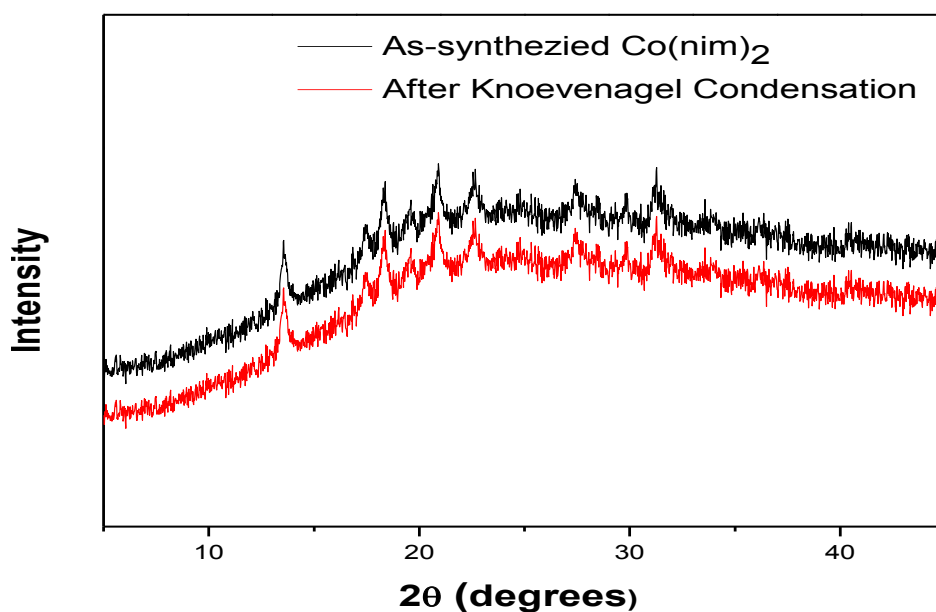


Figure 5. Comparison of PXRD pattern of fresh $\text{Co}(\text{nim})_2$ and after usage for specific organic synthesis reaction.

test. For $\text{Co}(\text{nim})_2$ diffraction patterns (Figure 5), the peaks of the used catalysts were maintained as fresh material, which demonstrates the stability of $\text{Co}(\text{nim})_2$ after usage as catalyst for Knoevenagel condensation.

Scanning electron microscope (SEM) shows a highly crystalline dipyrmaid (Figure 6a) and rhombic prism

(Figure 6b) shape crystals which confirmed the aforementioned crystal system specified by the Single Crystal X-ray analysis with a crystal sizes ranging approximately between 100 and 200 μm . Also, the optical micrograms confirmed the shape of the crystalline frameworks (Figure A in Supporting Appendix) which are

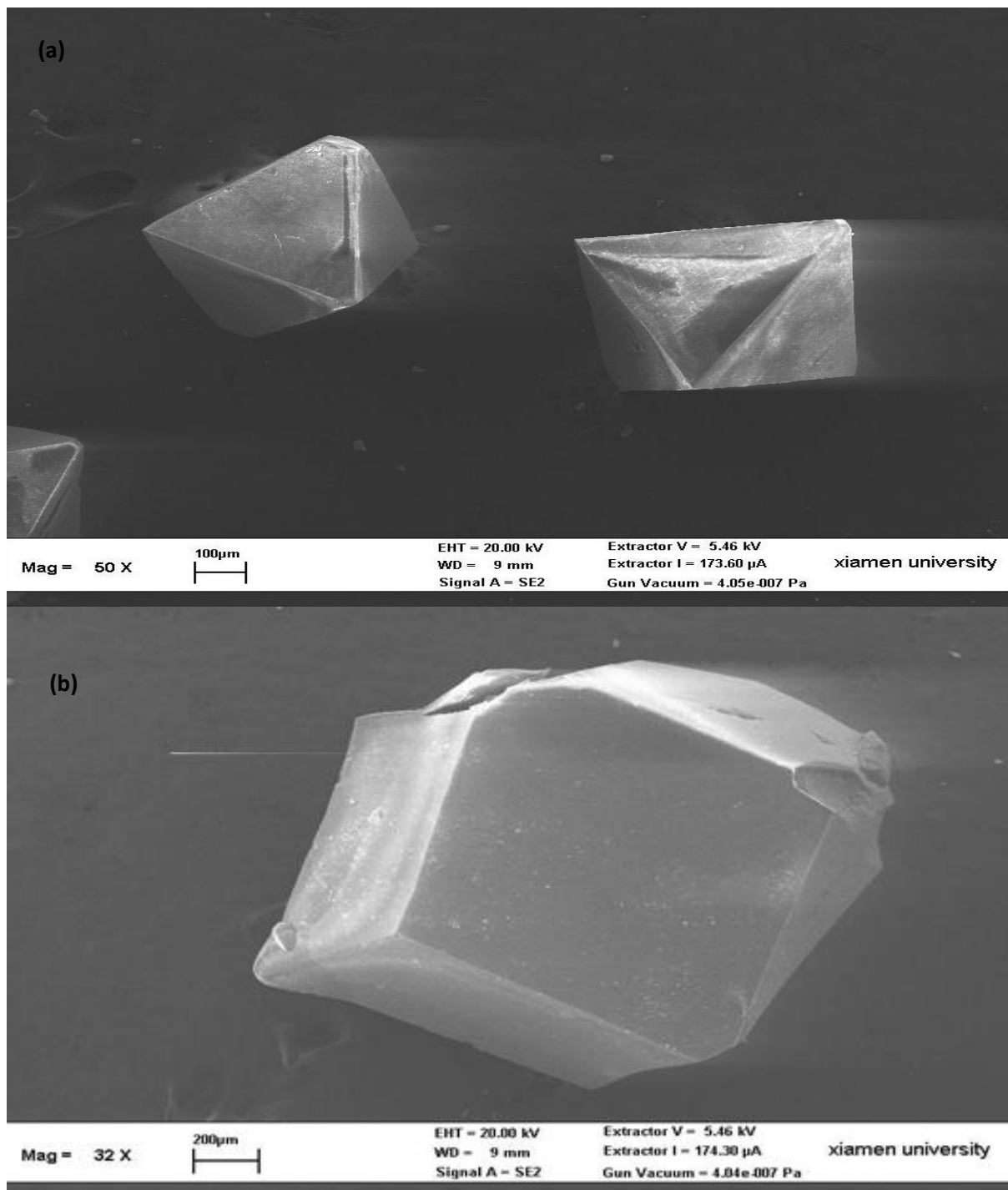


Figure 6. SEM micrograms of (a) $\text{Co}(\text{im})_2 \cdot 0.5\text{DMA}$ and (b) $\text{Co}(\text{im})_2 \cdot 0.5\text{DMF}$.

in agreement with previous reports on cobalt imidazolate frameworks (Tian et al., 2004; Banerjee et al., 2008).

Thermogravimetric analysis (TGA) shows weight loss of 8% up to 200°C corresponds to the release of guest molecules (0.5 DMA), and the most noteworthy feature in this result was found between the temperature range of

200 to 340°C with little weight loss, indicating that the $\text{Co}(\text{im})_2 \cdot 0.5\text{DMA}$ was stable up to 340°C (Figure 7). Afterward, a very rapid weight-loss step of 54% was observed as the temperature increased from 340 to 430°C demonstrating the thermal decomposition of the $\text{Co}(\text{im})_2 \cdot 0.5\text{DMA}$.

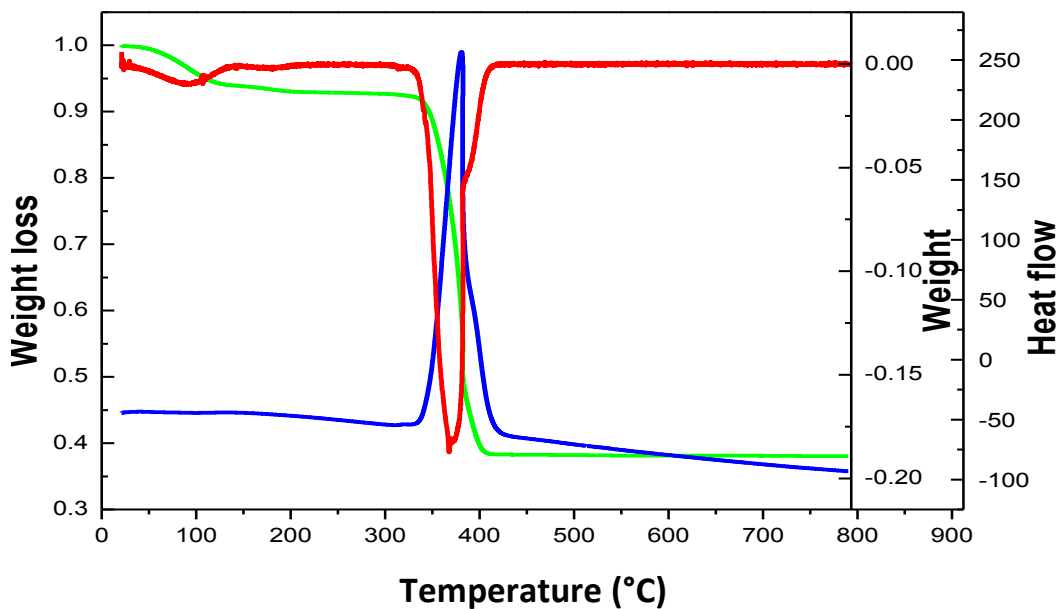


Figure 7. Thermogravimetric analysis (TGA) analysis of the $\text{Co}(\text{im})_2.0.5\text{DMA}$.

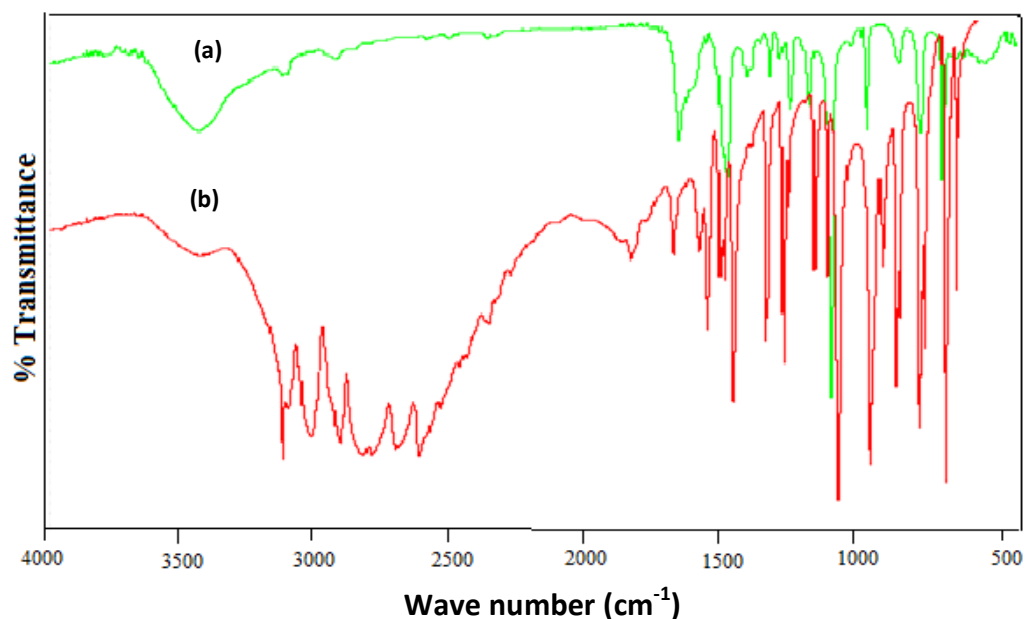


Figure 8. FT-IR spectra of (a) $\text{Co}(\text{im})_2.0.5\text{DMA}$ and (b) Imidazole.

Fourier transform infrared (FT-IR) spectra of $\text{Co}(\text{im})_2.0.5\text{DMA}$ alongside that of imidazole are shown in Figure 8. The presence of strong and broad N–H–N hydrogen bond was observed in the FT-IR spectra of imidazole ranging from 3350 to 2200 cm^{-1} with a maximum at about 2613 cm^{-1} and associated with weak band near 1830 cm^{-1} ; while the observed disappearance of these absorption bands evidently indicates the deprotonation of the

imidazole ligands during the formation of this porous crystalline framework (Corma et al., 2010). Besides, stretching vibrations of C–H bonds was observed near 3125 cm^{-1} and the double bond in the imidazole ring absorbs at 1650 cm^{-1} . Figure B1 in Supporting Appendix shows the FT-IR spectra of fresh $\text{Co}(\text{im})_2.0.5\text{DMA}$ along with used catalyst after specific organic transformation. In addition, the spectra for nitroimidazole along with fresh

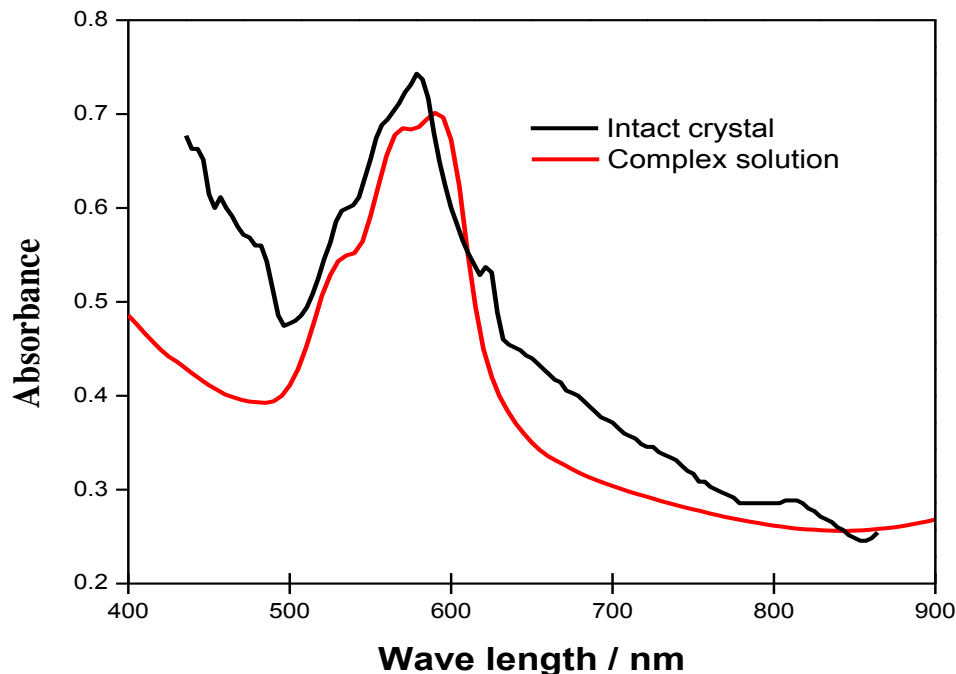


Figure 9. The UV-Vis spectra of $\text{Co}(\text{im})_2 \cdot 0.5\text{DMA}$ and that of the complex in solution.

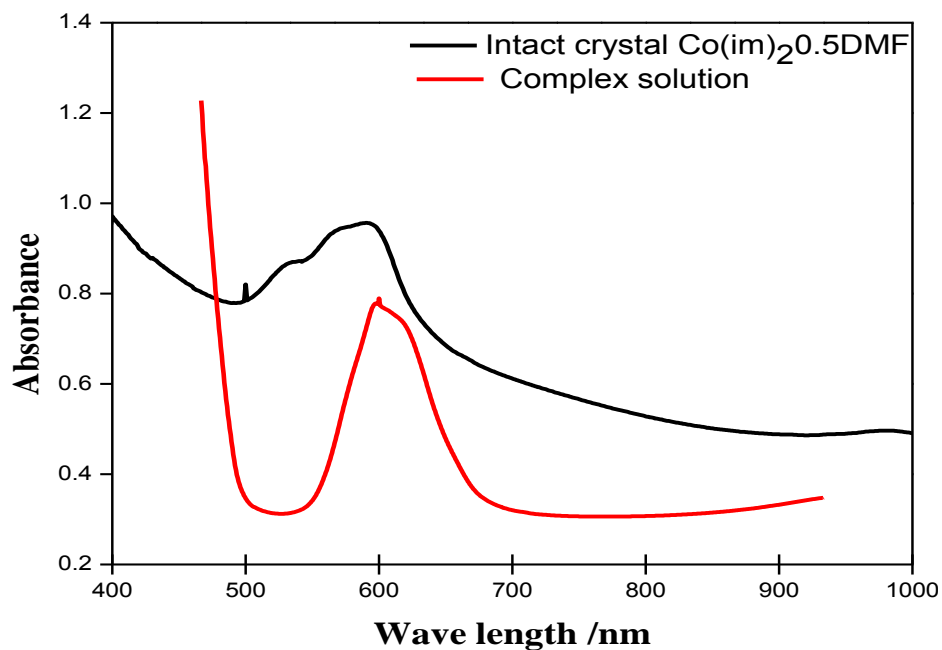


Figure 10. The UV-Vis spectra of $\text{Co}(\text{im})_2 \cdot 0.5\text{DMF}$ and that of the complex in solution.

and used $\text{Co}(\text{nim})_2$ are shown in Figure B2. Similar absorption bands were observed as $\text{Co}(\text{im})_2 \cdot 0.5\text{DMA}$ spectra with an inclusion of NO_2 stretching vibration near 1580 cm^{-1} .

In order to compare the UV-vis spectral properties of

the single crystal with that of the cobalt complex in solution, spectra of the solution was prepared in the same manner as the solution for crystal synthesis. As shown in Figures 9 to 11, the single crystal spectra do not differ very much in comparison with that of its complex

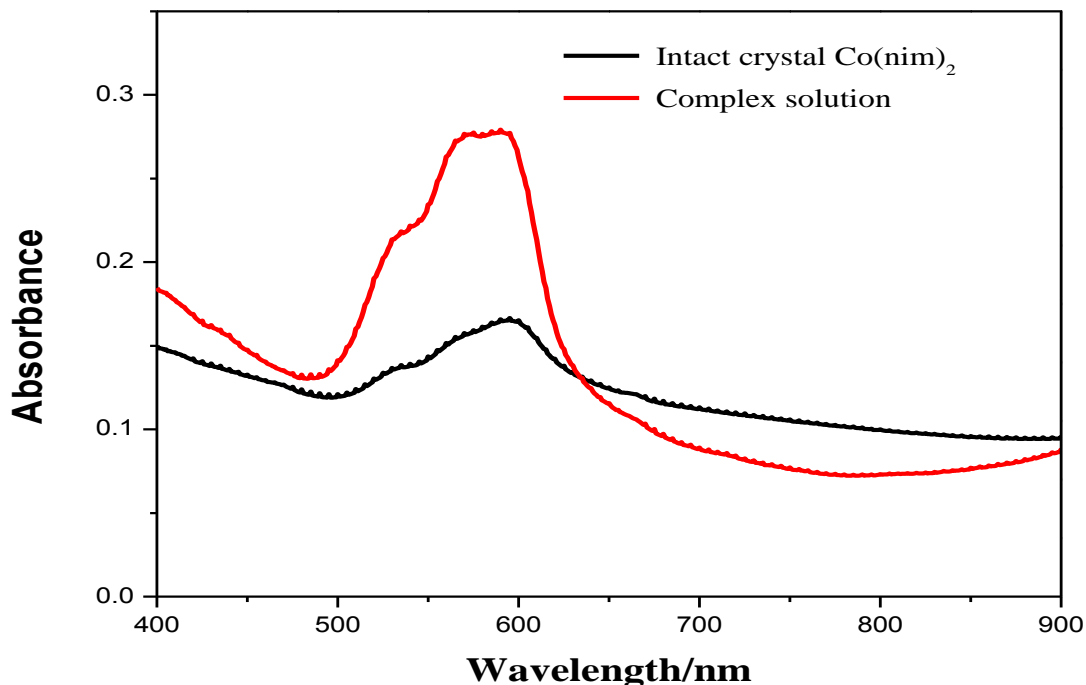


Figure 11. The UV-Vis spectra of $\text{Co}(\text{nim})_2$ and that of the complex in solution.

solution. The UV-Vis absorption spectra of the crystalline frameworks show several similar absorption bands, the maximum absorptions of $\text{Co}(\text{im})_2 \cdot 0.5 \text{DMA}$ (1), $\text{Co}(\text{im})_2 \cdot 0.5 \text{DMF}$ (2) and $\text{Co}(\text{nim})_2$ (3) are respectively about 600, 597 and 596 nm. These maximum can be assigned to the spin-allowed d-d transition $4A_2(F) \rightarrow 4T_2(P)$ of tetrahedral $\text{Co}(\text{II})$ ions (Lever, 1968; Poul et al., 2000); also a weak shoulder at about 535, 534 and 533 nm are observed respectively for the complexes. The λ_{max} of 1, 2 and 3 were hypsochromically shifted by about 10, 100 and 8 nm, respectively when compared with their complex solution.

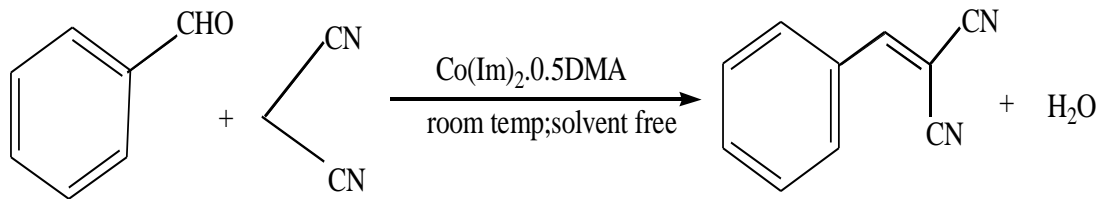
Catalytic activity of Co-ZIFs

Knoevenagel condensation

$\text{Co}(\text{im})_2 \cdot 0.5 \text{DMA}$ is accessed for its catalytic activity for Knoevenagel condensation reaction under a solvent free condition (Scheme 1). A conversion of 96% was obtained after 5 min, and the recovered catalyst was subsequently tested for reusability with an excellent conversion of 98%. Hence, while DCM was used as solvent with the same amount of reactants and catalyst; a conversion of 98% was achieved in 10 min without any significant change after three cycle of the catalyst (Figure 12). In good agreement with previous reports of Tran et al. (2011; Nguyen et al. (2012), Pande et al. (2005); using 5 mol % imidazole and the metal precursor ($\text{Co}(\text{NO}_3)_2 \cdot 6\text{H}_2\text{O}$)

instead of $\text{Co}(\text{im})_2 \cdot 0.5 \text{DMA}$ a 93% and 7% of quantitative conversion was achieved after 5 min. Since, both imidazole and $\text{Co}(\text{NO}_3)_2 \cdot 6\text{H}_2\text{O}$ can only act as homogenous catalysts which may not be practical from green perspective. To demonstrate that the catalytic activity of $\text{Co}(\text{im})_2 \cdot 0.5 \text{DMA}$ is devoid of any leached active species (imidazolate linkers), the reaction was carried out under solvent condition by using 5% mol of catalyst concentration, and then the reaction was stopped after 2 min filtered and analyzed by GC, and portion of the filtrate was transferred to another vial and stirred for further 5 and 8 min, respectively. During the 2 min, 57% conversion was obtained, and no further reaction and conversion was observed afterward while stirring further the filtrate. We then tested $\text{Co}(\text{nim})_2$ for Knoevenagel reaction with an initial conversion of over 90% obtained for both solvent free and solvent condition that took 20 and 30 min, respectively, and there was no observed loss of intrinsic catalytic activity after reusability test as shown in Figure 13.

Consequently, the slight lower conversion obtained with $\text{Co}(\text{nim})_2$ could be attributed to the base weakening influence of the nitro group on the imidazolate linker, however, $\text{Co}(\text{im})_2 \cdot 0.5 \text{DMA}$ is more basic with a corresponding higher conversion and shorter reaction time. The prominent active centers of Co-ZIFs are the basic sites (imidazolate linkers), with a plausible activity by Co^{2+} ions (Lewis acid sites) for Knoevenagel reaction as observed with $\text{Co}(\text{NO}_3)_2 \cdot 6\text{H}_2\text{O}$ when utilized as catalyst for this reaction. Although, Co^{2+} ions could



Scheme 1. Knoevenagel reaction of benzaldehyde with malononitrile using $[\text{Co}(\text{im})_2.0.5\text{DMA}]_\infty$ as catalyst.

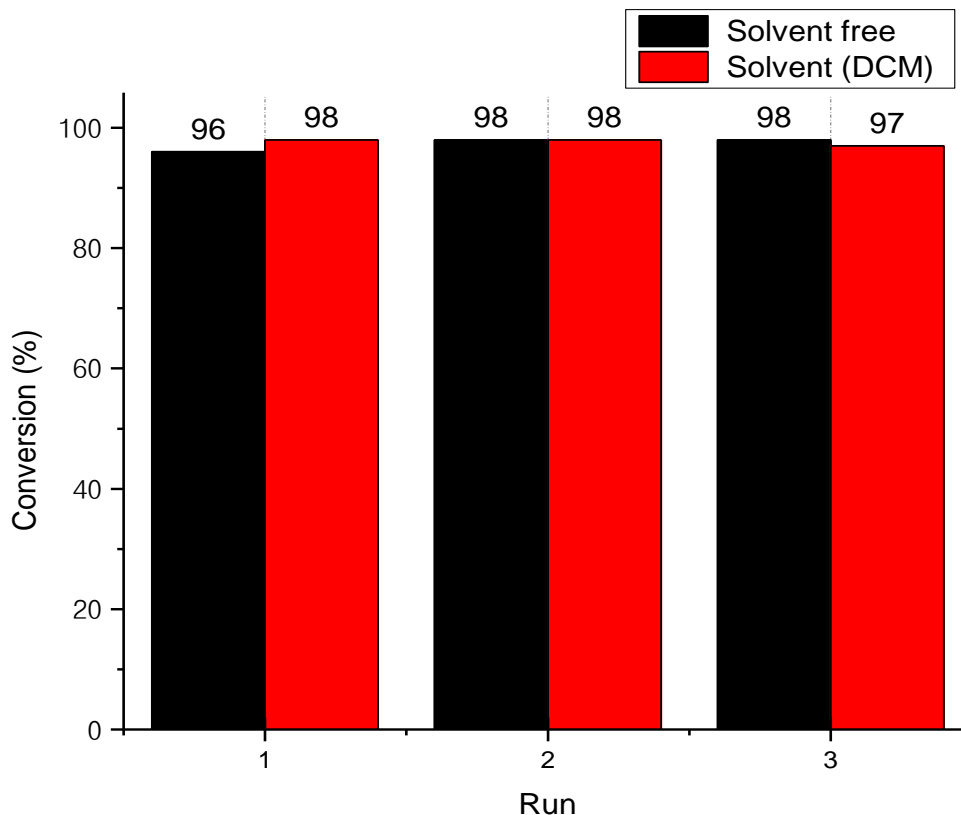


Figure 12. Catalyst reusability studies of $\text{Co}(\text{im})_2.0.5\text{DMA}$ with respect to conversion under solvent free and solvent condition.

activate the carbonyl substrates of the Knoevenagel condensation acting as catalyst or co-catalyst for the reaction (Gascon et al., 2009; Lladrés et al., 2012); markedly, the extra frameworks of CoO (impurities entrapped inside the pore cavities as either nanoparticles or segregated crystallites) also contribute to the catalytic activities of CO-ZIFs (Lladrés et al., 2012; Hafizovic et al., 2007; Calleja et al., 2010; Neogi et al., 2009). Comparative studies of the catalytic behaviour of Co-ZIFs with other state-of-the-art catalysts for the Knoevenagel condensation are shown in Table 1. We found that Co-ZIFs are efficient in the Knoevenagel condensation for the synthesis of benzylidene malononitrile. The conversions obtained with Co-ZIFs are higher than some previously obtained with Co-ZIFs; are higher than some previously

reported catalysts, where higher active methylene compounds moles were required for the same reaction and longer reaction time. Conversely, our catalysts exhibited less activity in the Knoevenagel condensation as compared to some base catalysts such as functionalized cobalt spinel ferrite and amine functionalized mesoporous zirconia (Tran et al., 2011; Phan and Jones, 2006; Parida et al., 2010).

Oxidation of ethylene glycol

In an effort to transform ethylene glycol to glycolic acid the catalytic prospect of this material was explored as

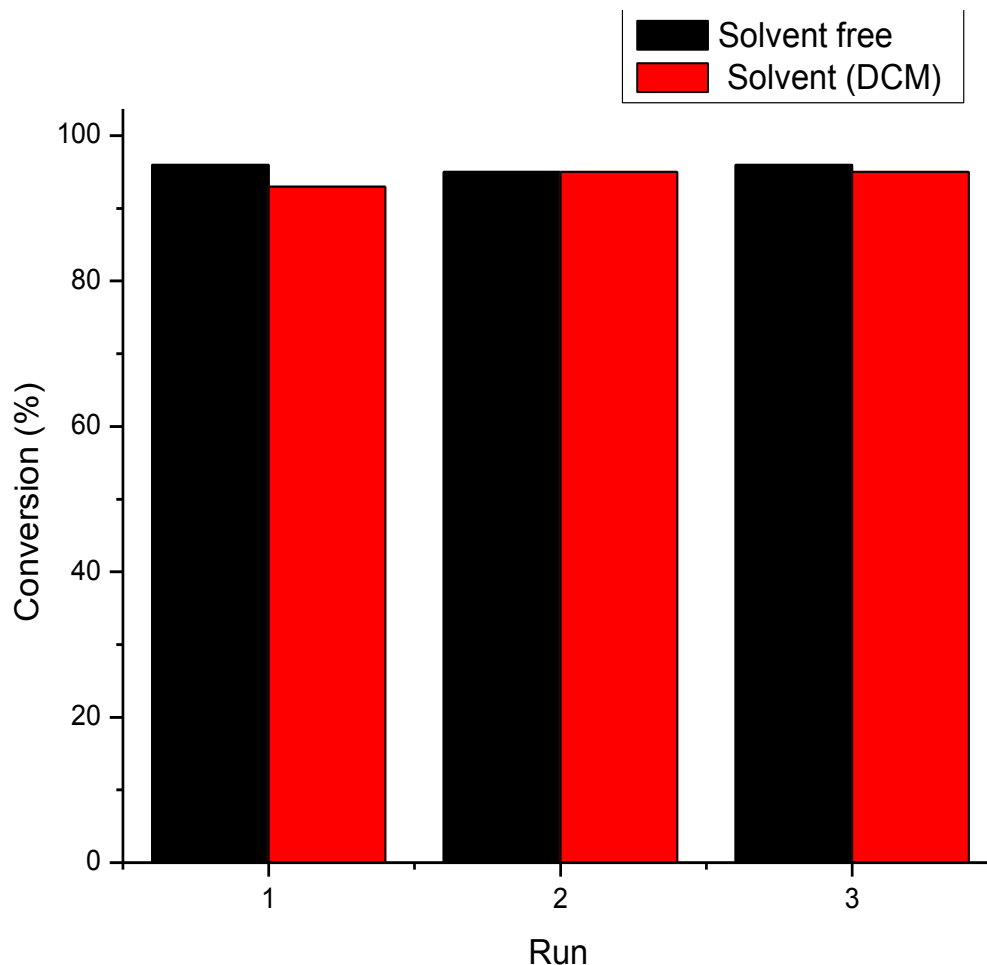
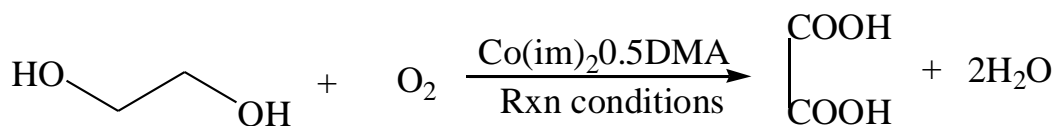


Figure 13. Catalyst reusability studies of $\text{Co}(\text{nim})_2$ with respect to conversion under solvent free and solvent condition.



Scheme 2. Catalytic oxidation of ethylene glycol using $\text{Co}(\text{im})_2 \cdot 0.5 \text{DMA}$ as catalyst.

shown in Scheme 2. The result obtained demonstrated the catalyst non-selectivity towards glycolic acid. In this case, ethylene glycol was totally oxidized to oxalic acid without any trace of glycolic acid, even when the reaction time and temperature was reduced to 30 min and 30°C , respectively (Table 2). We proposed that, to achieve a selective oxidation of ethylene glycol to glycolic acid, noble metal such as Au, Ag and Pt can be incorporated into the porous frameworks as metal ions or supported on it, since noble metals have been demonstrated to be effective for the selective conversion of EG to glycolic acid (Biella et al., 2002; Berndt et al., 2003).

Oxidation of ethylbenzene

In an effort to implement green principle in this chemical transformation procedure, the oxidation of ethylbenzene was carried out without using solvent and the oxidant employed was molecular oxygen. The $\text{Co}(\text{im})_2 \cdot 0.5\text{DMA}$ was found to be highly active and selective for the conversion of ethylbenzene to acetophenone. Hence, at temperature of 120°C and a pressure of $0.8 \times 10^6 \text{Pa}$, we observed 42% conversion of the substrate and a remarkable selectivity of 78.4% for acetophenone as shown in Scheme 3. As presented in Table 3, the results

Table 1. Comparative studies of the catalytic behaviour of Co(im)₂0.5 DMA) with other catalysts for Knoevenagel condensation.

Catalyst	Reaction conditions	Time (min)	Conversion/Yield	Reference
Diaminosilane-functionalized cobalt spinel ferrite (CoFe ₂ O ₄)	2.5 mol % of catalyst; Solvent: benzene; and at room temp; reactants mole ratio: malononitrile/benzaldehyde 2:1	5	100	Phan and Jones (2006)
ZIF-8	5 mol % catalyst, Solvent: Toluene; and at room temp; reactants mole ratio: malononitrile/benzaldehyde 4:1	120	100	Tran et al. (2011)
amine-functionalized mesoporous zirconia	1.79 mol % catalyst; Methanol; reactant mole ratio: and at room temp benzaldehyde/malonic ester 1:1	1440	89	Parida et al. (2010)
Guanidium lactate ionic liquid	2.5 mmol IL; and at room temp; reactants mole ratio: malononitrile/benzaldehyde 1:1	2	93 ^a	Xin et al. (2007)
In/AlMCM-41	0.06 mol % of In/AlMCM-41; under reflux condition in ethanol; reactants mole ratio: malononitrile/benzaldehyde 1.2:1	25	95 ^a	Katkar et al. (2010)
Co(im) ₂ 0.5DMA	10 mol % Catalyst; and at room temp; reactants mole ratio: malononitrile/benzaldehyde 1:1	5	98	This study
Co(nim) ₂	10 mol % Catalyst; and at room temp; reactants mole ratio: malononitrile/benzaldehyde 1:1	20	96	This study

a is product yield; T is this study, IL is ionic liquid.

for optimized reaction process for ethylbenzene oxidation are summarized. The conversion of ethylbenzene and its selectivity towards acetophenone increased rapidly from 42 to 71.3%, as temperature increased from 120 to 150°C. When the reaction time was increased from 2 to 10 h, initially both the conversion and selectivity of acetophenone increased and afterward no obvious change was observed due to inhibition by the product, while as a result of over oxidation of acetophenone or methylbenzylalcohol to benzoic acid the selectivity decreased gradually from 87.3 to 80.5%. As the pressure increased from 0.8 to 2.0 MPa, the conversion of the substrate and selectivity to acetophenone increased as well.

Likewise, the effect of catalyst concentration was studied, as the concentration Co-ZIF increased

from 0.04 to 0.2 mol, the conversion of substrate rapidly increased from 42 to 71.2% and acetophenone selectivity increased from 78.4 to 84.5%. Furthermore, the investigation of Co(nim)₂ and Co(NO₃)₂.6H₂O for catalytic oxidation of substrate under similar experimental condition, it was found that 40.3 and 39.4% of the ethylbenzene was converted to main product respectively, and a reasonable selectivity was obtained for both the crystalline porous framework and cobalt precursor.

Conclusion

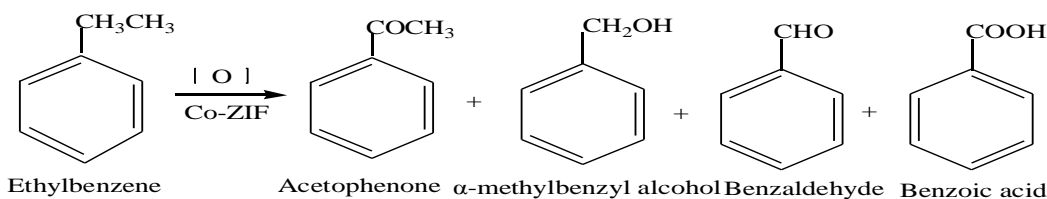
We examined Knoevenagel condensation of benzaldehyde using Co-ZIFs as catalyst for the

synthesis of benzylidene malononitrile under a solvent and solvent less condition with a remarkable conversion. The Co²⁺ of the coordination complex was explored for oxidation of ethylbenzene and ethylene glycol, since cobalt metal precursor was an important catalyst for oxidation transformation. As a result, the crystalline framework was not selective towards glycolic acid but oxidized the substrate to oxalic is less toxic. Moreover, Co-ZIF was found to be highly active for the oxidation of ethylbenzene and remarkably selective for acetophenone. This work accentuates the usefulness of MOFs as heterogeneous catalysts for organic synthesis, where either the metal ions or ligands can serve as catalyst for different organic transformations of interest.

Table 2. Catalytic oxidation of ethylene glycol using Co-ZIF as heterogeneous catalyst.

Catalyst (DMA)	Temp (°C)	Time (h)	Yield (%)
Co(im) ₂ 0.5	70	6	85
Co(im) ₂ 0.5	30	3	65
Co(im) ₂ 0.5	30	1 [†]	17
Co(im) ₂ 0.5	30	0.5	6.5

DMA is N,N-dimethylacetamide; reaction mixture with NaOH.

**Scheme 3.** Result of oxidation of ethylbenzene using Co(im)₂0.5 DMA as catalyst.**Table 3.** Catalytic oxidation of ethylbenzene under solvent less condition using Co-ZIFs as heterogeneous catalyst.

S/N	Reaction conditions	Conv (%)	Selectivity (%)			
			I	II	III	IV
1	120°C	42	78.4	15.5	0.7	5.4
2	130°C	57.5	79.5	13.8	0.6	6.1
3	140°C	67.8	83.6	12.1	0.7	3.6
4	150°C	71.3	84.5	7.8	0.5	7.2
5	4 h	70.4	87.3	6.1	0.6	6.0
6	6 h	70.8	86.5	5.7	0.5	7.3
7	8 h	71.3	81.4	4.9	0.4	13.3
8	10 h	71.5	80.5	4.1	0.4	15.0
9	1.5 Mpa	60.5	85.7	6.3	0.7	7.3
10	2.0 Mpa	67.4	87.8	5.4	0.5	6.3
11	0.08 mol	54.3	83.5	4.3	1.2	11
12	0.12 mol	59.5	83.9	4.5	0.8	10.8
13	0.16 mol	65.4	86.8	3.9	0.3	9
14	0.2 mol	71.2	84.5	3.1	0.3	12.1
15	Co(nim) ₂	40.3	78.7	15.1	0.6	5.6
16	Co(OAC) ₂ .6H ₂ O	39.4	69.1	18.3	2.4	10.2

ACKNOWLEDGEMENTS

We are grateful to the Chinese Government Scholarship Council and Xiamen University for providing necessary support during the course of this research. We also acknowledge one of the reviewers for helpful suggestions and comments.

Conflict of interests

The authors have not declared any conflict of interests.

REFERENCES

- Aijaz A, Xu Q (2014). Catalysis with Metal Nanoparticles Immobilized within the Pores of Metal–Organic Frameworks. *J. Phys. Chem. Lett.* 5(8):1400-1411.
- Banerjee R, Phan A, Wang B, Knobler C, Furukawa H, O’Keeffe M, Yaghi OM (2008). High-Throughput Synthesis of Zeolitic Imidazolate Frameworks and Application to CO₂ Capture. *Sci.* 319(5865):939-943.
- Berndt H, Pitsch I, Evert S, Struve K, Pohl MM, Radnik J, Martin A (2003). Oxygen Adsorption on Au/Al₂O₃ Catalysts and Relation to the Catalytic Oxidation of Ethylene Glycol to Glycolic Acid. *Appl. Catal. A.* 244(1):169-179.
- Biella S, Castiglioni GL, Fumagalli C, Pratia L, Rossi M (2002). Application of Gold Catalysts to Selective Liquid Phase Oxidation. *Catal. Today* 72(1-2):43-49.

- Calleja G, Botas JA, Orcajo MG, Sánchez-Sánchez M (2010). Differences between the isostructural IRMOF-1 and MOCP-L porous adsorbents. *J. Porous Mater.* 17:91-97.
- Chizallet C, Lazare S, Bazer-Bachi D, Bonnier F, Lecocq V, Soyer E, Quoineaud AA, Bats N (2010). Catalysis of Transesterification by a Nonfunctionalized Metal-Organic Framework: Acido-Basicity at the External surface of ZIF-8 Probed by FTIR and ab Initio Calculations. *J. Am. Chem. Soc.* 132(35):12365-12377.
- Corma A, García H, Llabrés FX, Xamena I (2010). Engineering Metal Organic Frameworks for Heterogeneous Catalysis. *Chem. Rev.* 110(8):4606-4655.
- Czaja AU, Trukhan N, Müller U (2009). Industrial Applications of Metal-Organic Frameworks. *Chem. Soc. Rev.* 38:1284-1293.
- Gascon J, Aktay U, Hernandez-Alonso MD, van Klink GPM, Kapteijn F (2009). Amino-based metal-organic frameworks as stable, highly active basic catalysts. *J. Catal.* 261(1):75-87.
- Gascon J, Corma A, Kapteijn F, Llabrés FX, Xamena I (2014). Metal Organic Framework, Catalysis: *Quo vadis?* *ACS Catal.* 4(2):361-378.
- Hafizovic J, Bjorgen M, Olsbye U, Dietzel PDC, Bordiga S, Prestipino C, Lamberti C, Lillerud KP (2007). The Inconsistency in Adsorption Properties and Powder XRD Data of MOF-5 Is Rationalized by Framework Interpenetration and the Presence of Organic and Inorganic Species in the Nanocavities. *J. Am. Chem. Soc.* 129(12):3612-3620.
- Kuppler RJ, Timmons DJ, Fang QR, Li JR, Makal TA, Young MD, Yuan D, Zhao D, Zhuang W, Zhou HC (2009). Potential Applications of Metal-Organic Frameworks. *Coord. Chem. Rev.* 253(23-24):3042-3066.
- Lee J, Farha OK, Roberts J, Scheidt KA, Nguyen ST, Hupp JT (2009). Metal-Organic Framework Materials as Catalysts. *Chem. Soc. Rev.* 38:1450-1459.
- Lever ABP (1984). *Inorganic Electronic Spectroscopy*. Elsevier, Amsterdam.
- Llabrés FX, Xamena I, Cirujano FG, Corma A (2012). An unexpected bifunctional acid base catalysis in IRMOF-3 for Knoevenagel condensation reactions. *Micro. Meso. Mater.* 157:112-117.
- Ma L, Lin W (2010). Designing metal-organic frameworks for catalytic applications. *Top Curr. Chem.* 293:175-205.
- Miralda CM, Macias EE, Zhu M, Ratnasamy P, Carreon MA (2012). Zeolitic Imidazole Framework-8 Catalysts in the Conversion of CO₂ to Chloropropene Carbonate. *ACS Catal.* 2(1):180-183.
- Nguyen LTL, Le KKA, Truong HX, Phan NTS (2012). Metal Organic Frameworks for Catalysis: The Knoevenagel Reaction Using Zeolite Imidazolate Framework ZIF-9 as an Efficient Heterogeneous catalyst. *Catal. Sci. Technol.* 2:521-528.
- Neogi S, Sharma MK, Bharadwaj PK (2009). Knoevenagel condensation and cyanosilylation reactions catalyzed by a MOF containing coordinatively unsaturated Zn(II) centers. *J. Mol. Catal. A: Chem.* 299(1-2):1-4.
- Pande A, Ganesan K, Jain AK, Gupta PK, Malhotra RC (2005). A Novel Eco-Friendly Process for the Synthesis of 2-Chlorobenzylidene malonitrile and its Analogues Using Water As a Solvent. *Org. Process Res. Dev.* 9(2):133-136.
- Parida KM, Mallick S, Sahoo PC, Rana SK, Facile A (2010). Method for Synthesis of Amine-Functionalized Mesoporous Zirconia and its Catalytic Evaluation in Knoevenagel Condensation. *Appl. Catal. A.* 381(1-2):226-232.
- Park KS, Ni Z, Cote AP, Choi JY, Huang R, Uribe-Romo FJ, Chae HK, O'Keeffe M, Yaghi OM (2006). Exceptional Chemical and Thermal Stability of Zeolitic Imidazolate Frameworks. *Proc. Natl. Acad. Sci. USA* 103(27):10186-10191.
- Phan NTS, Jones CW (2006). Highly Accessible Catalytic Sites on Recyclable Organosilane-Functionalized Magnetic Nanoparticles: An Alternative to Functionalized Porous Silica Catalysts. *J. Mol. Catal. A: Chem.* 253(1-2):123-131.
- Poul L, Jouini N, Fiévet F (2000). Layered Hydroxide Metal Acetates (Metal = Zinc, Cobalt, and Nickel): Elaboration via Hydrolysis in Polyol Medium and Comparative Study. *Chem. Mater.* 12(10):3123-3132.
- Santosh SK, Machhindra KL, Balasaheb RA, Sandip BR (2010). Indium Modified Mesoporous Zeolite AlMCM-41 as a Heterogeneous Catalyst for the Knoevenagel Condensation Reaction. *Bull. Korean Chem. Soc.* 31(5):1301-1304.
- Shekhar O, Liu J, Fischer RA, Wöll CH (2011). Mof Thin Films: Existing and Future Applications. *Chem. Soc. Rev.* 40:1081-1106.
- Tian YQ, Chen ZX, Weng LH, Guo HB, Gao S, Zhao DY (2014). Two Polymorphs of Cobalt(II) Imidazolate Polymers Synthesized Solvothermally by Using One Organic Template N,N-Dimethylacetamide. *Inorg. Chem.* 43(15):4631-4635.
- Tran UPN, Le KKA, Phan NTS (2011). Expanding Applications of Metal-Organic Frameworks: Zeolite Imidazolate Framework ZIF-8 as an Efficient Heterogeneous Catalyst for the Knoevenagel Reaction. *ACS Catal.* 1(2):120-127.
- Xin X, Guo X, Duan H, Lin Y, Sun H (2007). Efficient Knoevenagel Condensation Catalyzed by Cyclic Guanidinium Lactate Ionic Liquid as Medium. *Catal. Commun.* 8(2):115-117.
- Yilmaz B, Trukhan N, Müller U (2011). Industrial Outlook on Zeolites and Metal Organic Frameworks. *Chin. J. Catal.* 33(1):3-10.
- Zakzeski J, Dębczak A, Bruijninx PCA, Weckhuysen BM (2011). Catalytic Oxidation of Aromatic Oxygenates by the Heterogeneous Catalyst Co-ZIF-9. *Appl. Catal. A.* 394(1-2):79-85.
- Zhou X, Zhang HP, Wang GY, Yao ZG, Tang YR, Zheng SS (2013). Zeolitic imidazolate framework as efficient heterogeneous catalyst for the synthesis of ethyl methyl carbonate. *J. Mol. Catal. A: Chem.* 366:43-47.

APPENDIX

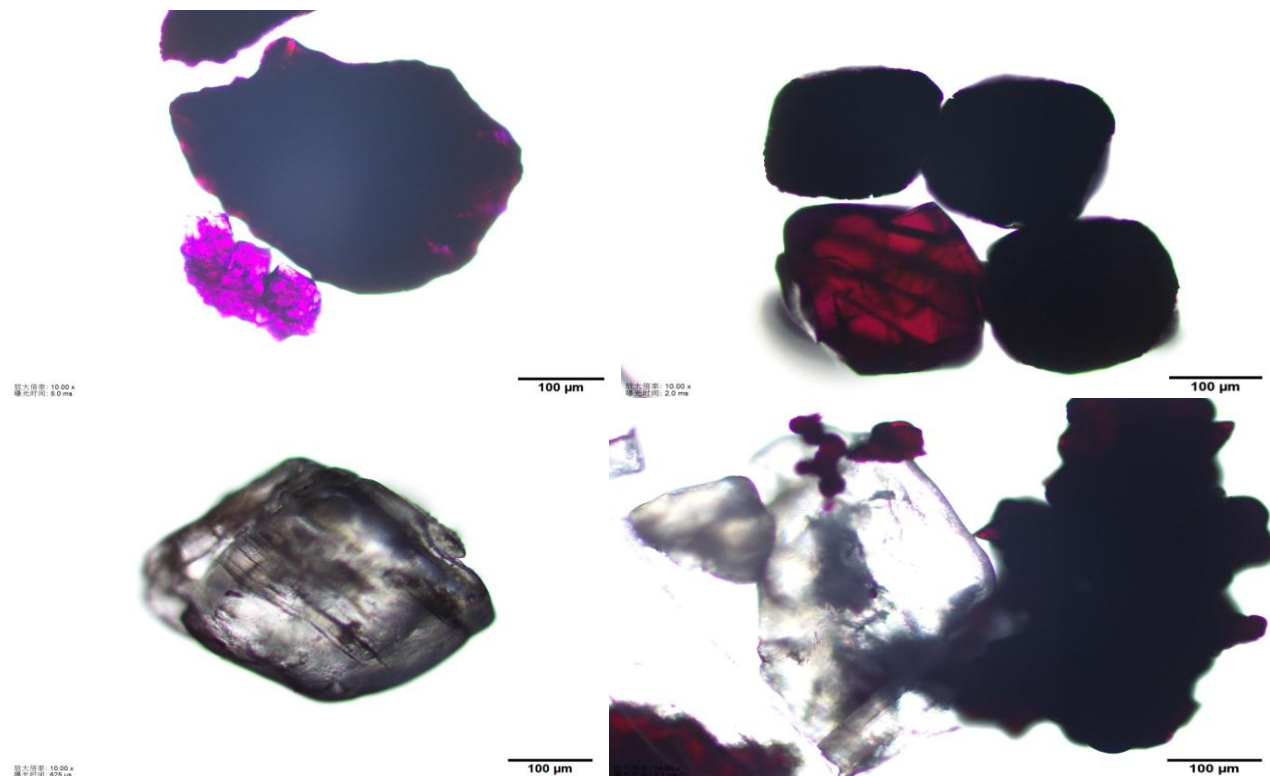


Figure A. Optical micrograms of (a) $\text{Co}(\text{im})_2\text{0.5DMA}$; (b) $\text{Co}(\text{im})_2\text{0.5DMF}$ and (c-d) $\text{Co}(\text{nim})_2$.

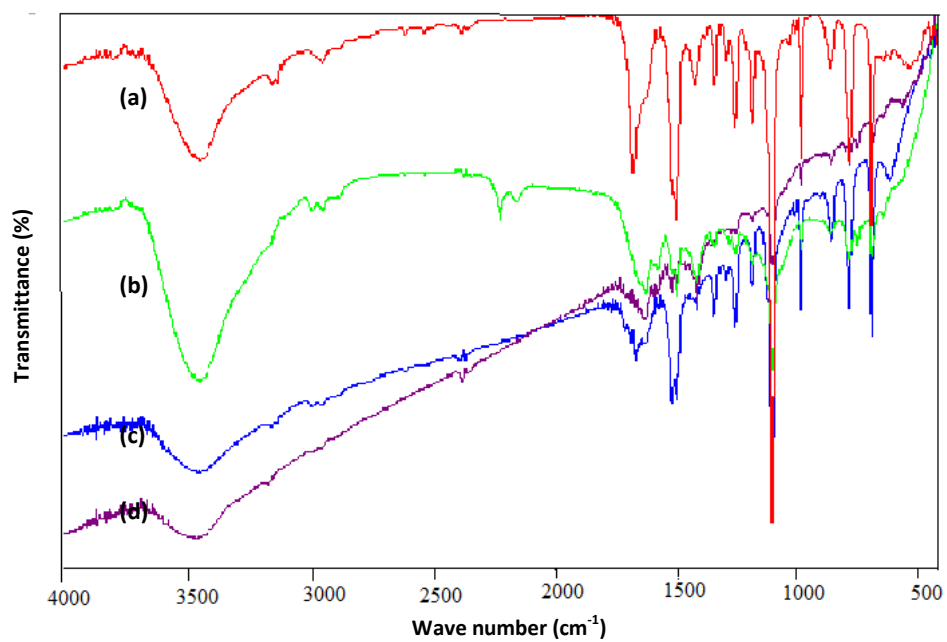


Figure. B1. FT-IR spectra of (a) fresh $\text{Co}(\text{im})_2\text{0.5DMA}$; after used for (b) Knoevenagel condensation (c) oxidation of Ethylbenzene and (d) ethylene glycol.

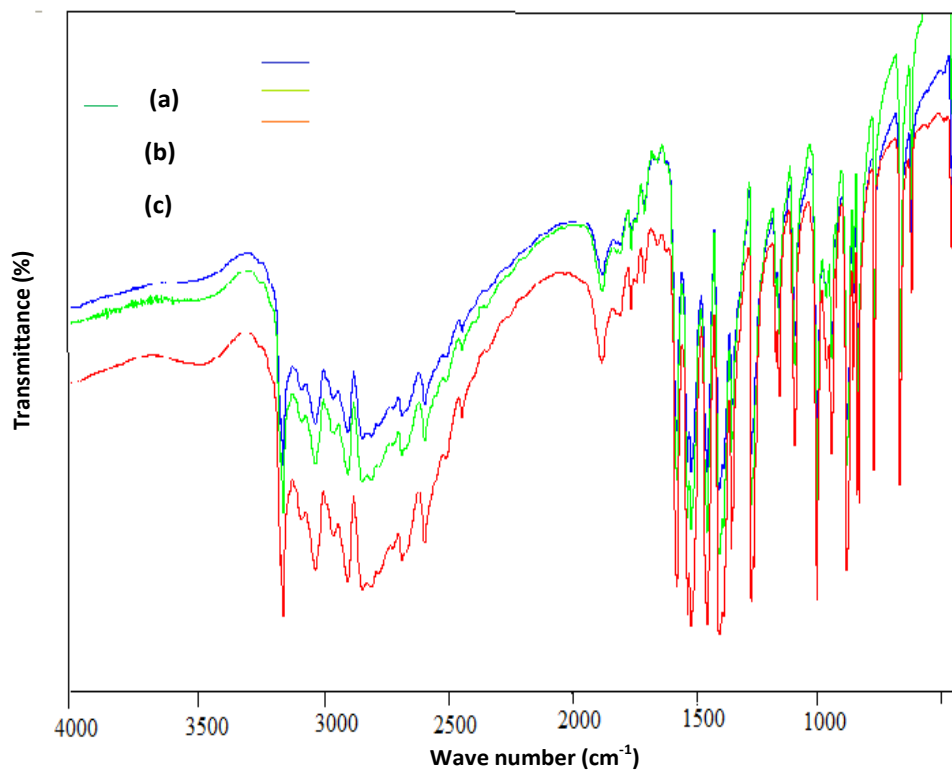


Figure B2. FT-IR spectra of (a) $\text{Co}(\text{nim})_2$; (b) after used as catalyst for Knoevenagel condensation; and (c) nitroimidazole.